UNIVERSITY OF BIRMINGHAM

Systematic identification of molecular mechanisms for aryl hydrocarbon receptor mediated neuroblastoma cell migration

Xu, Tuan; Luo, Yali; Xie, Heidi Qunhui; Xia, Yingjie; Li, Yunping; Chen, Yangsheng; Guo, Zhiling; Xu, Li; Zhao, Bin

Link to publication on Research at Birmingham portal

Full length article

Systematic identification of molecular mechanisms for aryl hydrocarbon receptor mediated neuroblastoma cell migration

Tuan Xu, Yali Luo, Heidi Qunhui Xie [*], Yingjie Xia, Yunping Li, Yangsheng Chen, Zhiling Guo, Li Xu, Bin Zhao [*]

State Key Laboratory of Environmental Chemistry and Ecotoxicology, Research Center for Eco-Environmental Sciences, Chinese Academy of Sciences, Beijing, China
University of Chinese Academy of Sciences, Beijing, China

ARTICLE INFO

ABSTRACT

Tumor cell migration is affected by the aryl hydrocarbon receptor (AhR). However, the systematic molecular mechanisms underlying AhR-mediated migration of human neuroblastoma cells are not fully understood. To address this issue, we performed an integrative analysis of mRNA and microRNA (miR) expression profiles in human neuroblastoma SK-*N*-SH cells treated with 2,3,7,8-tetrachlorodibenzo-p-dioxin (TCDD), a potent agonist of AhR. The cell migration was increased in a time- and concentration- dependent manner, and was blocked by AhR antagonist (CH223191). A total of 4,377 genes were differentially expressed after 24-hour-treatment with 10^{-10} M TCDD, of which the upregulated genes were significantly enriched in cell migration-related biological pathways. Thirty-four upregulated genes, of which 25 were targeted by 78 differentially expressed miRs, in the axon guidance pathway were experimentally confirmed, and the putative dioxin-responsive elements were present in the promoter regions of most genes (79 %) and miRs (82 %) in this pathway. Furthermore, two promigratory genes (*CFL2* and *NRP1*) induced by TCDD was reversed by blockade of AhR. In conclusion, AhR-mediated mRNA-miR networks in the axon guidance pathway may represent a potential molecular mechanism of dioxin-induced directional migration of human neuroblastoma cells.

1. Introduction

The aryl hydrocarbon receptor (AhR) is a ligand-dependent transcription factor that mediates the biological and toxic effects of dioxin exposure, in which dioxin binds to the AhR to form the dioxin-receptor complex and finally interacts with the dioxin responsive elements (DREs) in the promoter region to regulate the transcription of specific genes (Beischlag et al. 2008). AhR and AhR-dependent signaling pathways have been studied for decades because of not only their involvement in dioxin toxicity, the diversity of AhR ligands, but also the potential physiological functions of AhR, particularly in human tumors (Perepechaeva and Grishanova 2020; Xue et al. 2018). Neuroblastoma is one of the most common malignant tumors in infancy and early childhood (Park et al. 2010). Maternal exposure to dioxins has been proposed to correlate with the occurrence of neuroblastoma in children (aged 0–14 years) (Kerr et al. 2000). However, there is still a lack of direct evidence of a biological or toxicological link between dioxin exposure and neuroblastoma.

Tumor cell migration is one of the major factors leading to cancer progression. The AhR-dependent signaling pathway has been reported to play a role in regulating the migration of various tumor cells via regulating the expression of many migration-related genes (Hanieh 2015; Perepechaeva and Grishanova 2020; Zhu et al. 2020). However, activation of the AhR signaling pathway has diverse effects on cancer migration and invasion in lung, breast, and brain tumor cells (Jimma et al. 2019; Jin et al. 2014; Li et al. 2014; Peng et al. 2009; Yamaguchi and Hankinson 2019). Our previous study has shown that the spontaneous motility of human neuroblastoma cells is significantly reduced under the complete culture condition after treatment with 2,3,7,8-tetrachlorodibenzo-p-dioxin (TCDD), the most potent dioxin congener (Luo

---

et al. 2020). However, under low serum culture condition, the expression of the promigratory gene cell division cycle 42 (*CDC42*) is significantly increased (Xu et al. 2018). Thus, the effect of dioxins on the spontaneous and directional movement of neuroblastoma cells may lead to inconsistent or even opposite outcomes. AhR has been shown to mediate the expression of certain genes involved in the migration of cancer cells, such as *CDC42* (Xu et al. 2018) and matrix metalloproteinase-1 (*MMP1*) (Villano et al. 2006). Therefore, we hypothesize that the AhR-dependent signaling pathway and its downstream genes may be important factors in revealing the molecular events in dioxin-treated neuroblastoma cells. By using mRNA microarray analysis in the perinatal mouse brain after fetal exposure to dioxins, Mitsui et al. observed that the significant upregulation of two inflammatory chemokines (*CXCL4* and *CXCL7*) might be the transcriptional mechanism underlying the development of neurobehavioral alterations caused by dioxins (Mitsui et al. 2011). Thus, revealing alterations in AhR-dependent mRNA expression profiles may help outline the molecular basis of the relationship between dioxin exposure and neuroblastoma at the transcriptional level (Fujita et al. 2006; Mitsui et al. 2011).

MicroRNAs (miRs) are a class of ∼ 22 nucleotide small noncoding RNAs that are important posttranscriptional regulators of gene expression by inhibiting mRNA translation or promoting mRNA degradation. Our previous study identified 277 differentially expressed miRs in TCDD-treated (10^{-10} M) human neuroblastoma cells using a miR microarray analysis (Xu et al. 2017). Furthermore, AhR and upregulated *miR-608* coregulate *CDC42* expression, which provides insights into the molecular mechanism of dioxin-induced neurotoxicity at the transcriptional and posttranscriptional levels (Xu et al. 2017). Compared with a single mRNA-miR association study, a systematic and integrative analysis of mRNA and miR expression profiles might provide additional biological insights into the biological pathways associated with phenotypic traits of interest (Long et al. 2013; Van der Goten et al. 2014). Given the roles of AhR in dioxin-induced mRNA and miR expression alterations, such a systematic and integrative analysis will be able to comprehensively reveal the molecular basis underlying the cellular effects of dioxin on neuroblastoma cells.

In this study, a relatively low concentration of TCDD, which is close to the median serum level of dioxins in exposed populations in Vietnam, and Seveso Italy (Eskenazi et al. 2002; The Tai et al. 2011; Xie et al. 2013), was administered to SK-*N*-SH cells to activate the AhR in an environmentally relevant way, and the effects on human neuroblastoma cell migration were revealed. An integrative analysis of mRNA and miR transcriptomes was conducted to identify potential molecular mechanisms at both transcriptional and posttranscriptional levels. The roles of AhR in TCDD-induced cellular effects and expression of related representative genes were revealed by using an AhR antagonist. This study provided a systematic approach to explore the toxicological mechanisms of dioxins, as well as many testable hypotheses on the effect of dioxins on human neuroblastoma.

2. Materials and methods

2.1. Cell culture

The SK-*N*-SH cell line was obtained from the Cell Resource Center of the Chinese Academy of Medical Sciences (Beijing, China) and was routinely grown in Dulbecco's Modified Eagle's Medium (DMEM, Gibco, Life Technologies, Melbourne, Australia) supplemented with 10 % fetal bovine serum from an Australian source (FBS, Corning) and a mixture of 100 U/ml penicillin with 100 μg/ml streptomycin (1 % P/S; Gibco, Life Technologies). Cells were grown at 37 °C in a humidified incubator with 5 % CO_2.

2.2. Exposure experiments

Cells were seeded in culture dishes at an appropriate density and incubated for 24–36 h. After reaching 70 % confluence, cells were exposed to TCDD. TCDD was purchased from Wellington Laboratories Inc. (Ontario, Canada) and dissolved in dimethyl sulfoxide (DMSO, Sigma-Aldrich, Canada). TCDD was employed at low concentrations of 5×10^{-11}, 10^{-10} and 2×10^{-10} M. DMSO was present at 0.1 % or lower in all groups. CH223191, an inhibitor of the AhR-dependent pathway, was obtained from Sigma (St. Louis, MO, USA) and used at a concentration of 10^{-6} M. After treatment, cells were washed with phosphate-buffered saline (PBS, pH 7.4) twice for gene microarray and other experiments.

2.3. Scratch motility assay

SK-*N*-SH cells were seeded into 6-well plates and grown to 100 % confluence in complete culture medium. The monolayers of confluent cells were scratched with a sterile pipette tip and washed with PBS twice to remove the floating cells. Cells were then incubated with serum-free medium to exclude the effect of cell proliferation. For the detection of concentration-dependent effects, cells were exposed to 5×10^{-11}, 10^{-10} and 2×10^{-10} M TCDD or 0.1 % DMSO for 48 h. For the detection of time-dependent effects, cells were exposed to 10^{-10} M TCDD or 0.1 % DMSO for 24 h, 36 h and 48 h. Photographs of the initial wound and the movement of the cells in the scratched area were captured using an inverted light microscope at 100 × magnification (Olympus CKX41, Tokyo, Japan). Six invariant fields along the initial wound area were randomly selected from each well image and subsequently imaged. The initial and resulting wound areas in the selected fields were quantified using Image-Pro Plus 6.0 software (Media Cybernetics, Bethesda, MD, USA). The cell migration distance was calculated as the area divided by the length of each selected field (He et al. 2007; Li et al. 2015).

2.4. Transwell migration assay

The migration of the SK-*N*-SH cells was quantified using a 24-well Transwell chamber with an 8 μm pore size polycarbonate membrane (Costar, NY, USA). SK-*N*-SH cells were seeded into each upper chamber at a density of approximately 5×10^4 per well and incubated with TCDD or 0.1 % DMSO in serum-free medium. Complete medium with TCDD or 0.1 % DMSO was added to each corresponding bottom chamber for chemoattraction. For the detection of concentration-dependent effects, cells were exposed to 5×10^{-11}, 10^{-10} and 2×10^{-10} M TCDD or 0.1 % DMSO for 48 h. For the detection of time-dependent effects, cells were exposed to 10^{-10} M TCDD or 0.1 % DMSO for 24 h, 36 h or 48 h. After the incubation, nonmigrating cells were removed from the upper surface of the upper chamber membrane with a wet cotton swab. Cells that had migrated across the membrane to the lower surface were fixed with a solution containing methanol: glacial acetic acid = 3:1 and stained with a 0.1 % crystal violet solution for 5 min. Then, the membrane was extensively washed with water and air-dried at room temperature. An hour later, the membrane was carefully isolated, mounted using neutral balsam, and covered with cover slips. Photographs of stained cells were captured under an inverted light microscope (Olympus CKX41) at 400 × magnification with a digital camera. The number of migrated cells was counted using Image-Pro Plus 6.0 software (Media Cybernetics). The average number of cells from at least four random fields per membrane was considered the number of migrated cells.

2.5. mRNA microarray analysis

Total RNA was extracted from cell samples using the TRIzol/chloroform method and then purified with magnetic beads from Agencourt Ampure (Beckman Coulter, Brea, CA, USA). Target preparation for microarray processing was performed according to the instructions provided with the GeneChip® WT PLUS Reagent Kit. In each preparation, 500 ng of total RNA were used for two rounds of cDNA synthesis. After fragmentation of 2nd-cycle single-stranded cDNAs, the samples were labeled with biotin using terminal deoxynucleotidyl transferase

(TdT) and then hybridized to a GeneChip® Human Transcriptome Array 2.0 (HTA 2.0, Affymetrix, Santa Clara, CA, USA) with 44,699 annotated genes for 16–18 h at 45 °C. Following hybridization, the microarrays were washed and stained with streptavidin phycoerythrin on an Affymetrix Fluidics Station 450. Microarrays were scanned using the Affymetrix® GeneChip Command Console (AGCC) installed in a GeneChip® Scanner 3000 7G. Scanned images (.CEL format) were imported into Affymetrix Expression Console software (version 1.4.1) (Affymetrix, Santa Clara, CA, USA) for normalization with the Robust Multichip Average (RMA) algorithm, and the generated normalized data files were imported into Affymetrix Transcriptome Analysis Console (TAC) 3.0 Software (Affymetrix, Santa Clara, CA, USA) to identify differentially expressed genes.

2.6. Gene ontology (GO) and kyoto encyclopedia of genes and genomes (KEGG) enrichment analysis

The upregulated or downregulated genes from the mRNA microarray were separately subjected to GO (https://geneontology.org/) and KEGG (https://www.genome.jp/kegg/) enrichment analyses using the package "clusterProfiler" in R (version 3.8.1) (Yu et al. 2012). GO terms or KEGG pathways with p value < 0.05 were considered statistically significant.

2.7. Quantitative Real-Time PCR (qRT-PCR)

Total RNA was extracted from SK-*N*-SH cells using the RNAprep PurePure Cell/Bacteria Kit (Tiangen Biotech Co., ltd., Beijing, China) according to the manufacturer's instructions. Total RNA (2.5 μg) was reverse transcribed using a Thermo Scientific RevertAid First Strand cDNA Synthesis Kit (Thermo Fisher Scientific) according to the manufacturer's instructions. The expression of genes was quantified by qRT-PCR using the GoTaq® qPCR Master Mix kit according to the manufacturer's instructions (Promega, Madison, WI, USA). The SYBR green signal was detected using a LightCycler 480 Instrument (LC-480II, Roche). The qRT-PCR conditions were as follows: 5 min at 95 °C, followed by 45 cycles each consisting of 10 s at 95 °C, 20 s at 60 °C and 30 s at 72 °C, and a cooling step of 16 s at 42 °C. The data were analyzed using the ΔΔCt method. 18S rRNA was used as an internal control for quantification. The sequences of primer pairs with GenBank accession numbers are provided in the supplementary information (Table S1).

2.8. Putative promoter regions of genes and miRs

Differentially expressed genes were hierarchically clustered using the ward. D2 agglomeration method within the "pheatmap" package in R. The putative promoter sequences (2000 bp) of the selected gene sets were retrieved utilizing the "TxDb.Hsapiens.UCSC.hg38.knownGene" Bioconductor package in R. The number and location of potential DREs were visualized using the "ggplot2" package in R. The promoters of miRs were predicted based on the miRStart database (https://mirstart.mbc.nctu.edu.tw/).

2.9. Network analysis of miRs and target genes

The interaction between differentially expressed genes and miRs induced by TCDD was retrieved using the "multiMiR" package (version 1.18.0) in R, which provided access to three validated miR-target gene databases (miRTarBase, miRecords, and TarBase) (Ru et al. 2014). The identified miR-target gene pairs were used to construct regulatory networks and visualized using the "igraph" package in R.

2.10. Statistical analysis

All experiments except the microarray were repeated independently at least three times, and all data are presented as the means ± SEM.

Statistical analyses were performed using IBM SPSS 19.0 software (IBM Corp., Armonk, NY). We used one-way analysis of variance (ANOVA) and the Bonferroni correction for all analyses. We considered p value < 0.05 as a statistically significant difference.

3. Results

3.1. TCDD enhanced directional cell migration via AhR

We examined the time- and concentration- dependent effects of TCDD on the migration of neuroblastoma cells. Two migration-related cellular assays, the scratch motility assay and Transwell migration assay, were conducted under the serum-starved conditions.

In the scratch motility assay, the initial width and area of the wounds in all treated groups were similar (Table S2). Cells in both the DMSO control and TCDD groups gradually migrated across the wounds (Fig. 1A). Throughout the observation period, none of the cell groups achieved 100 % wound closure. Notably, 5×10^{-11} M TCDD had no effect on cell migration (Fig. 1B). Cells exposed to 10^{-10} and 2×10^{-10} M TCDD for 48 h migrated a longer distance compared to cells in the control group (Fig. 1B), and the additional migration distance was similar in these two groups (Table S3). The lower concentration, 10^{-10} M TCDD, was used for the subsequent time course experiments. Cells were viable for up to 48 h after wounding under serum starvation conditions. Therefore, we focused on an observation window of 24–48 h and found that the TCDD treatment accelerated cell migration over this time period (Fig. 1C). Compared to the corresponding controls, the additional migration distance gradually increased in the TCDD-treated groups over time: the 36 and 48 h treatment groups had significantly longer additional migration distances than the 24 h group (Table S3). Based on these results, TCDD promoted the migration of SK-*N*-SH cells after the generation of a scratch wound in a time- and concentration- dependent manner. Similar induction effects were observed in the Transwell migration assay. More cells migrated to the other side of the membrane after 48 h of treatment with all TCDD concentrations (5×10^{-11}-2×10^{-10} M) compared to the control (Fig. 2A). In addition, more cells migrated in the 10^{-10} M and 2×10^{-10} M TCDD groups than in the 5×10^{-11} M TCDD group (Fig. 2B). However, no significant difference was observed between the 10^{-10} and 2×10^{-10} M TCDD groups (Fig. 2B). Regarding the time course response, 48 h of TCDD treatment elicited a more apparent induction of cell migration than 24 and 36 h of treatment (Fig. 2C). These time- and concentration- dependent effects suggested that the Transwell migration assay was more sensitive to low concentrations of TCDD treatment (5×10^{-11} M) than the scratch motility assay. However, a longer time (48 h) was needed to observe the effects.

CH22319, a ligand-selective antagonist of AhR that preferentially inhibits the effects of TCDD (Zhao et al. 2010), was employed to assess the role of AhR in the induction of cell migration. Cell migration was significantly increased after 24 h of treatment with 10^{-10} M TCDD in either the scratch motility assay or the Transwell migration assay (Fig. 1D & 2D). In contrast, pretreatment with CH223191 blocked this induction, indicating that AhR was involved in dioxin-induced cell migration (Fig. 1D & 2D).

3.2. TCDD alters the gene expression profile

We investigated the effects the gene expression profile to explore the molecular mechanism of TCDD-induced cell migration. The mRNA microarray analysis was performed on the cells after 24 h of treatment with 10^{-10} M TCDD or 0.1 % DMSO. The data revealed 4,377 differentially expressed genes ($p < 0.05$), including 2,539 upregulated and 1,838 downregulated genes (Table S4 and Fig. 3A). At low concentrations, TCDD significantly altered the expression of a large number of genes, but most of the changes were moderate. Among all differentially expressed genes, 368 upregulated and 533 downregulated genes exhibited changes greater than 20 % compared to the control. Only 3 upregulated and 5
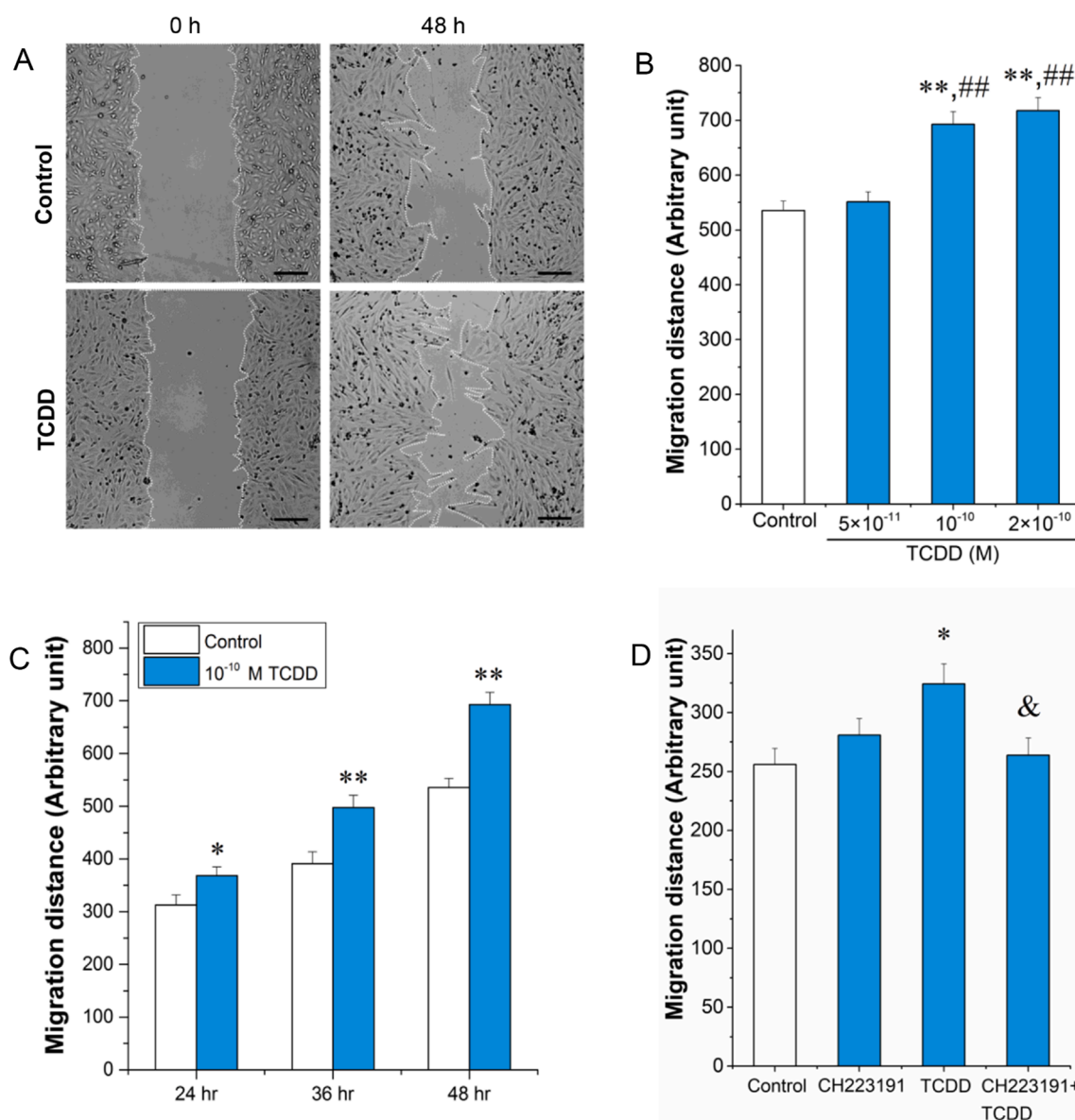
Fig. 1. Effects of TCDD on cell migration in the scratch motility assay. Representative images (A) were captured at $100 \times$ magnification (scale bar $= 200$ μm). The concentration response (B) and time course (C) studies were performed with the AhR inhibitor (D). Values are presented as the means $\pm$ SEM from triplicate samples in three independent experiments. Statistical analyses were performed using one-way ANOVA with the Bonferroni test. $^*p < 0.05$ compared with the control group. $^{**}p < 0.01$ compared with the control. $^{##}p < 0.01$ compared with 5×10^{-11} M TCDD. $^{\&}p < 0.05$ compared with the TCDD group.

downregulated genes exhibited a greater than 2-fold change (Table S4). All normalized data have been deposited in the Gene Expression Omnibus database (GEO; https://www.ncbi.nlm.nih.gov/geo/; accession number GSE101464).

3.3. Functional analysis of differentially expressed genes

We performed GO and KEGG pathway enrichment analyses of up- and downregulated genes, respectively. Fifty-two KEGG pathways and 64 GO terms were significantly enriched by the upregulated genes, while 40 KEGG pathways and 250 GO terms were enriched by the downregulated genes (Tables S5, S6, S7, and S8). The effect of TCDD on inducing cell migration may be due to upregulation of a series of promigratory genes. Six KEGG pathways and 2 GO terms (one biological process and one cellular component) in which the upregulated genes were enriched were closely related to cell migration (Fig. 3B). The axon guidance pathway was associated with the other seven functionally enriched GO terms and KEGG pathways (Fig. 3B). Detailed information

on the functionally enriched terms and pathways was presented in Tables S5, S6 and S9.

3.4. Verification of the expression of axon guidance Pathway-Related genes and their targeting miRs

The expression of almost all genes was consistent with the microarray results, showing an increasing trend compared to the control (Fig. 4A). For example, upon exposure to 10^{-10} and 2×10^{-10} M TCDD, the levels of Cofilin 2 (*CFL2*) and Neuropilin 1 (*NRP1*) mRNAs were significantly increased in SK-*N*-SH cells, consistent with the mRNA microarray data (Fig. 4A). The lowest concentration of TCDD (5×10^{-11} M) had no effect on the expression of *CFL2* and *NRP1* (Fig. 4A). Among the three experimental concentrations, the 10^{-10} M treatment exerted the maximum effect on inducing *CFL2* and *NRP1* expression (Fig. 4A). Because the 10^{-10} M and 2×10^{-10} M groups did not show any significant difference, we used 10^{-10} M TCDD for the time course experiments. We observed significant increases in the expression of *CFL2* and *NRP1* after
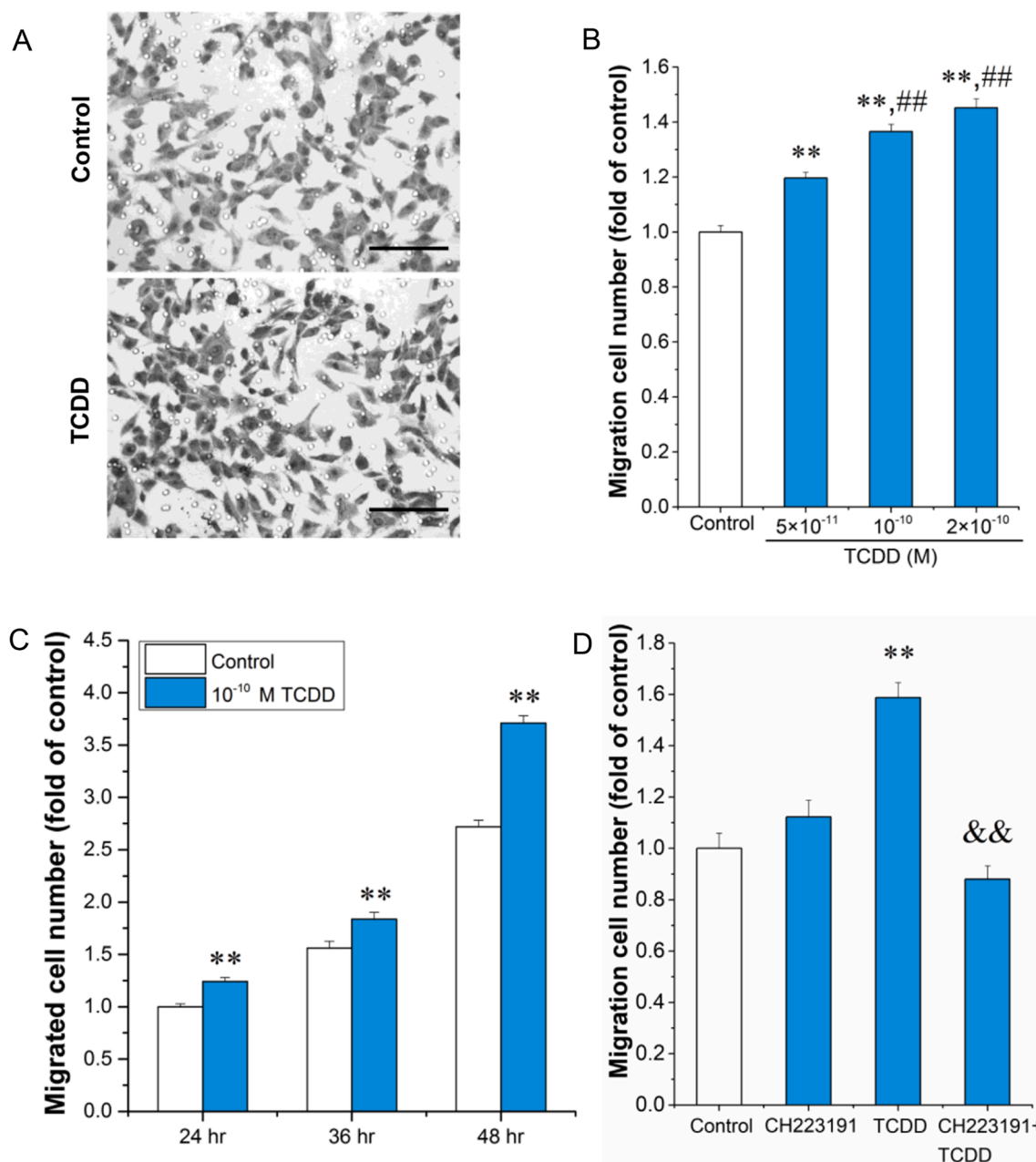
Fig. 2. Effects of TCDD on cell migration in the Transwell migration assay. Representative images (A) were captured at 400 × magnification (scale bar = 100 μm). The concentration response (B) and time course (C) studies were performed with AhR inhibitors (D). Values are presented as the means ± SEM from triplicate samples in three independent experiments. Statistical analyses were performed using one-way ANOVA with the Bonferroni test. $**p < 0.01$ compared with the control. $^{\#\#}p < 0.01$ compared with 5×10^{-11} M TCDD. $^{\&\&}p < 0.01$ compared with the TCDD group.

24, 36 and 48 h of exposure to 10^{-10} M TCDD compared with controls, but no significant difference was observed between the time points for TCDD-treated groups (Fig. 4A). Only a few genes were downregulated at a certain time point or after exposure to different concentrations, such as *MET* expression at 48 h of exposure to 2×10^{-10} M TCDD (Fig. 4A). The relative expression of genes in the axon guidance pathway was grouped into 8 clusters, and *CDC42*, *NRP1* and *CFL2* were in the same cluster (Fig. 4A). Some downregulated genes identified in the microarray assay were also involved in the axon guidance pathway (Figs. S1 and S2A). We integrated axon guidance pathway-related genes and their targeting miRs to obtain more precise information on the molecular events related to the genes whose expression was altered by TCDD. Among the 34 upregulated genes in the axon guidance pathway, twenty-five genes and their targeting 78 miRs (50 upregulated and 28 downregulated miRs)

are shown in Fig. 4B and Table S9. Nine genes (*EPHB3*, *PPP3CC*, *SEMA6D*, *BMPR1B*, *UNC5C*, *NRP1*, *CXCL12*, *PTCH1*, and *MET*) were targeted by only one miR, and the other 16 genes were targeted by multiple miRs (Fig. 4B and Table S9). Except for *SEMA4F* and *PIK3R1* (which were only related to downregulated miRs), the others (23 genes) were linked to both up- and downregulated miRs (Fig. 4B).

3.5. Potential DREs of axon guidance Pathway-Related genes and their targeting miRs

The promoter regions of genes in the axon guidance pathway were predicted, and the DRE sequences present therein were identified to study the potential mechanism by which TCDD altered gene expression. In addition to *WNT5A*, *PLXNA4*, *NRAS*, *PIK3R1*, *UNC5C*, *PLXNA2* and
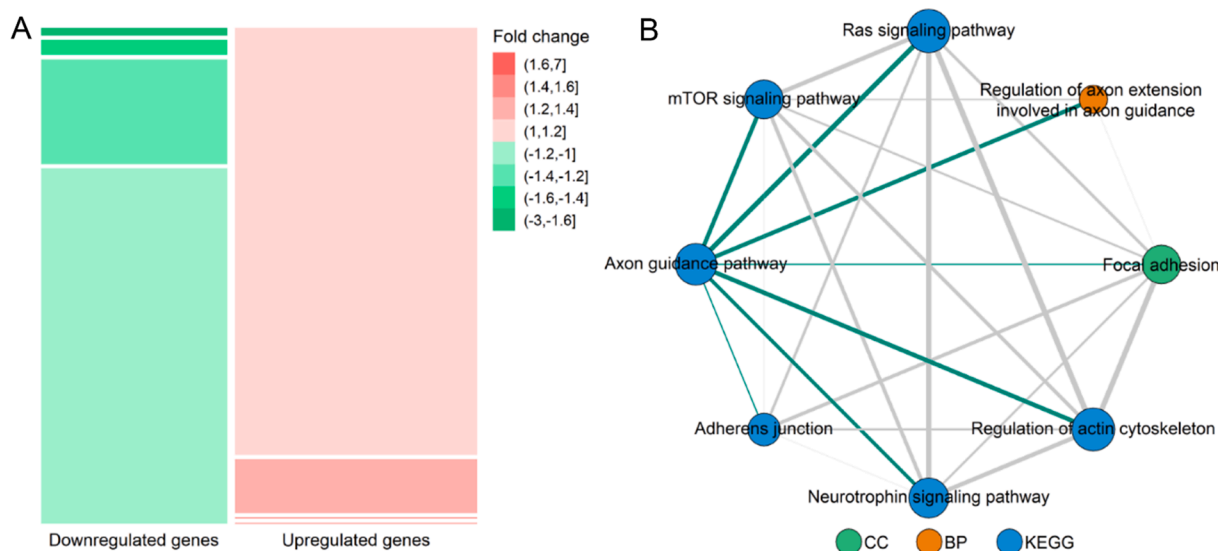
Fig. 3. The effect of TCDD on gene expression profile. (A) The mosaic plot shows the distribution of differential expression profiles. The columns represent up- or downregulated classes of gene expression. The area of three rectangle is proportional to the number of genes identified under each condition. The colors represent the range of fold changes. (B) The network plot shows the interrelationship of cell migration-related functional clusters. The node size represents the number of genes in each functional cluster, and the color represents different types of functional clusters. The edge thickness represents the number of overlapping genes between each cluster.
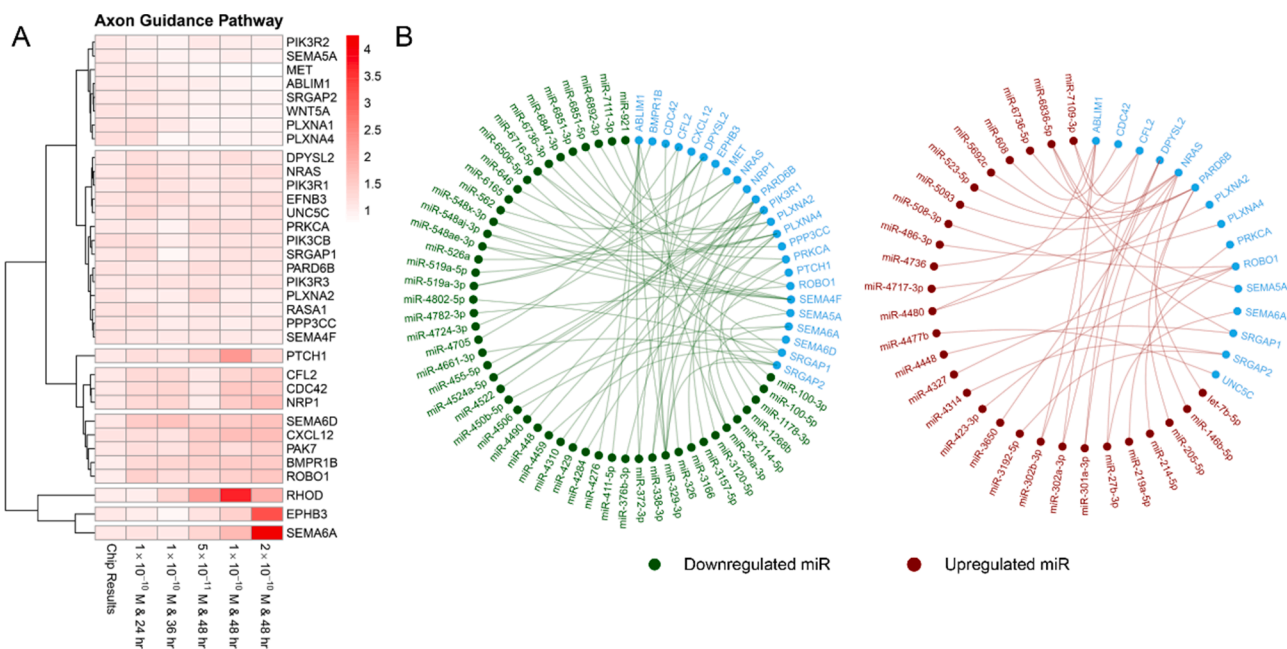

Fig. 4. The differentially expressed genes and their targeting miRs in the axon guidance pathway. (A) Hierarchical cluster of gene expression in the axon guidance pathway. Each row in the heat map represents a gene, and each column represents a treatment. Colors represent the level of gene expression. (B) Interaction network of differentially expressed miRs and their target genes in the axon guidance pathway.

BMPR1B, other genes (27 genes) contained different numbers of DRE sequences (ranging from 1 to 8), and these DREs were closely or sparsely distributed in the corresponding promoter regions (Fig. 5A). The details of the downregulated genes in the axon guidance pathway were provided in the supplementary information (Fig. S2B). Pretreatment with CH223191 blocked the induction of *CFL2* and *NRP1* expression, indicating that AhR was involved in TCDD-induced gene expression (Fig. 5B). The DRE distribution in the promoter regions of miRs was detected using a bioinformatics analysis (Fig. 5C). The top three miRs ranked by the number of DREs were, were *miR-455-5p* (11 DREs), *miR-6836-5p* (10 DREs), and *miR-4717-3p* (9 DREs). The number of DREs was

not obviously different between up- and downregulated miRs.

4. Discussion

Our scratch motility assay showed that TCDD induced a significant increase in the directional migration of SK-*N*-SH cells, and these findings were further supported by the Transwell migration assay (Figs. 1 and 2). Similar evidence of human cell migration in response to dioxin has been reported for the HepG2 hepatoblastoma cell line (Bui et al. 2009), A2058 melanoma cell line (Villano et al. 2006), MCF-7 breast cancer cell line (Seifert et al. 2009), and U937 monocytic cell line (Vogel et al.
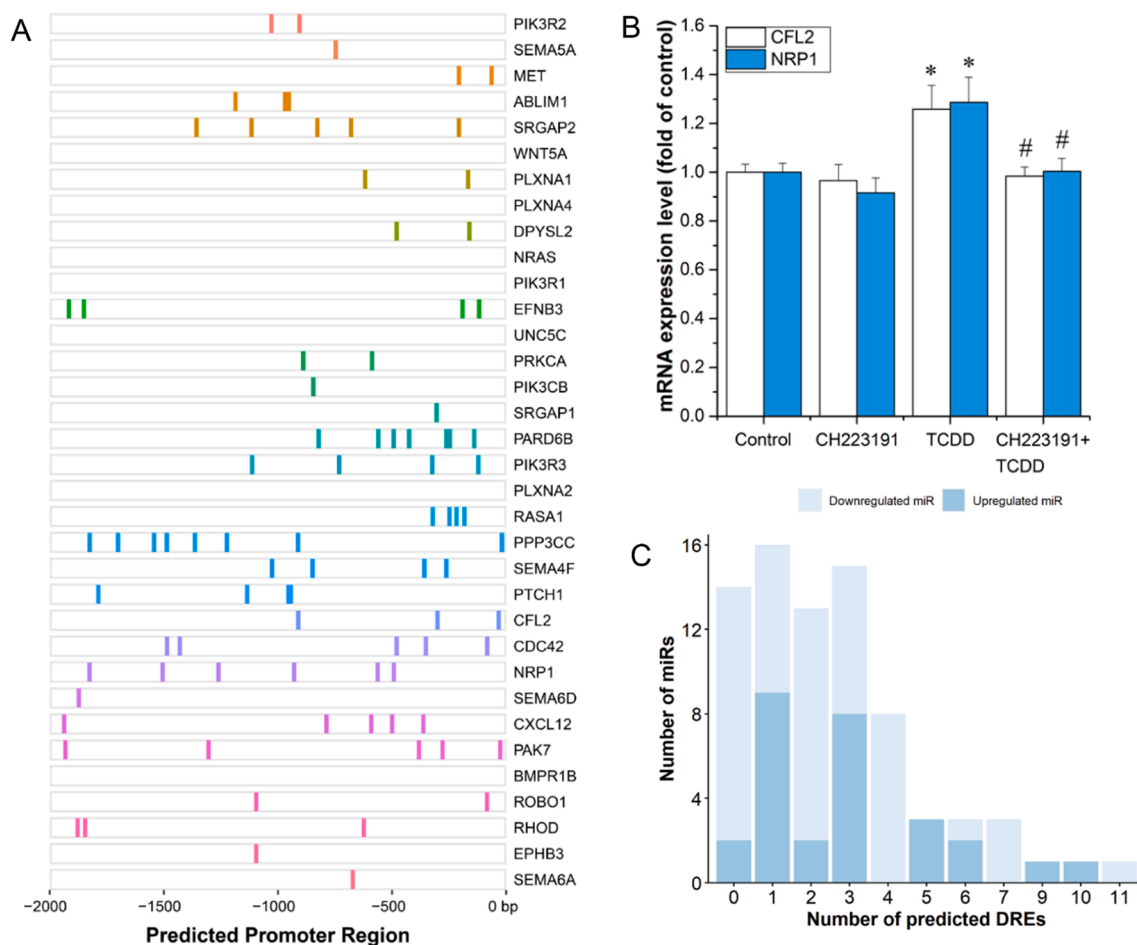
Fig. 5. DREs in the predicted promoter regions of differentially expressed genes and targeting miRs in the axon guidance pathway. (A) The number and location of DREs in the gene promoters. Each bar represents one DRE sequence. (B) Verification of DREs in the promoters of the *CFL2* and *NRP1* genes. Values are presented as the mean ± SEM from triplicate samples in three independent experiments. Statistical analyses were performed using one-way ANOVA with the Bonferroni test. *$p < 0.05$ compared with the control group. #$p < 0.05$ compared with the TCDD group. (C) The number of predicted DREs in miR promoters.

2004). As shown in our previous study, TCDD affects the spontaneous movement of SK-*N*-SH cells under full nutrient conditions (Luo et al. 2020). The results from our study can serve as an experimental validation for the hypothesis that low concentrations of TCDD can promote human neuroblastoma cell migration, which also provided support for an alternate explanation for the impact of environmental exposure to dioxins on the health of the nervous system(Kim et al. 2010). AhR is a ligand-activated transcription factor that mediates the expression of a diverse set of promigratory genes in response to dioxins, and these promigratory genes participate in distinct signaling pathways to ultimately achieve a common output of cell migration, which was confirmed by our results (Fig. 1D and Fig. 2D). Due to its advantages of simplicity and economy, the scratch motility assay is one of the traditional and classical method used to assess cell migratory ability in vitro monolayer culture of cells (He et al. 2007; Li et al. 2015). No obvious change in SK-*N*-SH cell viability has been reported after exposure to such low concentrations of TCDD (Xie et al. 2013). In addition, another classical method, the Transwell migration assay was also performed to verify that the effect of TCDD on promoting cell migration, showing consistent results from the scratch motility assay (Figs. 1 and 2).

A systematic analysis is an efficient approach to investigate the potential molecular mechanisms of directional cell migration induced by TCDD. The initial observations of TCDD-induced cell migration in SK-*N*-SH cells prompted us to focus on the upregulated genes, and the axon guidance pathways enriched by these genes may be an important molecular mechanism involved in AhR-mediated transcriptional and miR-

mediated posttranscriptional regulation. The microarray analysis provided valuable clues to the molecular mechanisms of dioxin-induced cell migration. Our study produced a novel dataset of alterations in the neuronal mRNA expression profile in response to exposure to low concentrations (10^{-10} M) of TCDD (Table S4 and Fig. 3). To our knowledge, no comparable dataset has been reported under similar TCDD treatment conditions in a human-derived neuronal system. In this mRNA microarray data, most differentially expressed genes exhibited moderate but significant changes, among which only 49 of 4,377 differentially expressed genes exhibited greater than 50 % changes compared to the control. Similar moderate changes (<2-fold change) in dioxin-induced gene expression have been observed in other human-derived cells in vitro, such as HepG2 cells, in which TCDD treatments at much higher concentrations (10^{-9} M) were employed (Frueh et al. 2001). McHale et al. investigated the global gene expression profile in peripheral blood mononuclear cells of 26 dioxin-exposed Seveso individuals (McHale et al. 2007). When comparing the highly exposed subjects with individuals exposed to background TCDD levels (average plasma levels were 99.4 and 6.7 ng/L, respectively), the majority of the top 50 significantly altered genes (*p* value < 0.05) showed low levels (<20 %) of up- or downregulation (McHale et al. 2007). Thus, using similar exposure levels (10^{-10} M) to dioxin, we set the *p* value < 0.05 as the cutoff to determine the differentially expressed genes from the mRNA microarray data in the present study. Three hundred sixty-eight upregulated and 533 downregulated genes displayed a greater than 20 % change compared to the control (Table S4). Differentially expressed

genes are commonly used to dissect various cellular and molecular mechanisms of the adverse health effects of environmental pollutants. Gandhi et al. found that exposure to excess levels of manganese (10^{-4} M) induces alterations in the gene expression profile of human SH-SY-5Y neuroblastoma cells, and these genes were involved in multiple neuronal pathways, such as neuron differentiation and development, regulation of neurogenesis, synaptic transmission, and neuronal cell death (apoptosis) (Gandhi et al. 2018). Pang et al. identified 794 differentially expressed genes in bisphenol A-treated PC12 cells, and these genes were involved in fundamental metabolic processes under physiological and pathological conditions (Pang et al. 2018). Although the alterations in the expression of most genes in our study were moderate, the changes in the expression of these genes might lead to significant alterations in cell signaling and biological functions (Tables S5, S6, S7, and S8).

Cell migration is governed by a complex network of signaling pathways and molecular elements. Some KEGG pathways and GO terms were associated with cell migration (Fig. 3B). Cell migration and axon guidance both result from cytoskeletal modifications triggered by the similar axon guidance proteins, which are involved in neurogenesis and neuronal differentiation processes (Van Battum et al. 2015). Thus, we hypothesized that the axon guidance pathway might explain the migration of quiescent neuroblastoma cells. The expression of upregulated genes in the axon guidance pathway was validated using qPCR (Fig. 4A). Consistent with our previous study (Xu et al. 2018), *CDC42* expression was significantly increased. Two genes (*NRP1* and *CFL2*) were significantly increased in a time- and concentration- dependent manner (Fig. 4A). *NRP1* is a non-tyrosine kinase receptor for vascular endothelial growth factor that modulates the migration of glioma cells and non-nervous cancer cells (Evans et al. 2011; Jia et al. 2010; Yin et al. 2015). In addition, TCDD treatment upregulates *NRP*1 expression in the HepG2 cells, consistent with our finding. *CFL2* is one of the components of the Rho-kinase pathway, and its overexpression is closely related to the progression of glioblastoma multiforme (GBM) and patient survival (Erkutlu et al. 2013). *CFL2* might be one of the downstream effector genes of the promigratory effect, and it has not been reported as a dioxin-responsive gene. Since AhR has been proposed to crosstalk with this small Rho GTPase pathway to physiologically control cell migration via this cytoskeleton regulator, it might be indirectly involved in the *CDC42*-related regulation of *CFL2*. The roles of AhR in mediating *CDC42* upregulation by TCDD further support this hypothesis (Xu et al. 2017).

MiRs play a crucial role in the regulation of cell migration in the nervous system. Wang et al. showed that *miR-608* significantly attenuated the migration of glioma stem cells by negatively regulating the expression of macrophage migration inhibitory factor (MIF) at the posttranscriptional level by targeting its 3′-untranslated regions (Wang et al. 2016). *CDC42* is a small GTPase of the Rho family that is involved in cytoskeletal reorganization and cell migration and motility. As shown in our previous study, *miR-608*-related posttranscriptional mechanisms are involved in the regulation of *CDC42* expression in dioxin-treated neuroblastoma cells (Xu et al. 2017). One hundred and three miR-target gene pairs were identified in the present study, providing potential evidence for the posttranscriptional regulation of promigratory genes in SK-*N*-SH cells by dioxins (Fig. 4B). The expression of these miRs was significantly altered by TCDD, suggesting that miRs are required for gene expression in the axon guidance pathway.

AhR plays a central role in dioxin-induced toxicity, and most of these processes appear to depend on the binding of AhR to DREs within the promoter regions of target genes. The presence of DRE core sequences (5′- GCGTG- 3′) in the promoter region is a common feature of classical dioxin-responsive genes. Most differentially expressed genes in the axon guidance pathway contain DREs in their promoter regions (Fig. 5A), indicating that these genes may be regulated by AhR. For example, TCDD may directly regulate the expression of *CFL2* via AhR-dependent transcriptional regulation since 3 DREs were identified in the *CFL2* promoter (Fig. 5A). Similarly, the presence of 6 DREs in the *NRP1*

promoter also supports this hypothesis. The effects of pretreatment with the AhR antagonist CH223191 on inhibiting the TCDD-induced upregulation of *NRP1* and *CFL2* further support the AhR-dependent transcriptional regulatory mechanism described above (Fig. 5B). The induction of miR expression is also regulated by transcription factors acting in trans on the promoter regions of miRs. DREs were also identified in the promoter regions of most axon guidance pathway-related miRs (Fig. 5C), suggesting that AhR may indirectly regulate cell migration through miRs. For example, six DREs are present in the promoter region of *miR-301a-3p*, the expression of which was upregulated by dioxins in our previous miR microarray study, and it enhanced cell migration in the pancreatic ductal adenocarcinoma cells and colorectal cancer cells (Xia et al. 2015; Zhang et al. 2019). Similarly, the presence of 3 DREs in the promoter region of *miR-329-3p* inhibited the migration of gastric cancer cells (Li et al. 2015), the expression of which was downregulated by dioxins in our previous study (Xu et al. 2017).

In our study, we found that TCDD was able to induce SK-*N*-SH cell migration by a potential mechanism of AhR-mediated differential expression of mRNAs and miRs. In addition, TCDD may also cause some subcellular structural changes that are associated with cell migration. For example, Diry et al., found that dioxin treatment led to significant changes in the morphology of epithelial cells, remodeling their cytoskeleton to increase the interaction with extracellular matrix as well as loosening cell-to-cell contacts (Diry et al. 2006). Bui et al. found that dioxin treatment could dramatically change HepG2 cell shape and focal adhesion sites number via AhR signaling pathway (Bui et al. 2009). Therefore, further experimental verification on the effects of TCDD on subcellular structure (e.g., in situ expression of some cytoskeleton factors) are still needed in the future studies. In order to visualize the process, the downstream responses (i.e., some subcellular structural changes) caused by dioxin were complemented by literature text mining in the Gene Reference into Function (GeneRIF) database. Finally, we provided a schematic map that is similar to the adverse outcome pathway (AOP) framework, including two molecular initiating events (i. e., differentially expressed miRs and genes), two key events (i.e., KEGG signaling pathway/GO term, and downstream responses), and an adverse outcome (i.e., cell migration) (Fig. S3). The flow chart not only complemented the existing AOP framework related to neurotoxicity, but also provided clues to investigate the mechanism of TCDD cytotoxicity.

5. Conclusions

In summary, low concentrations of TCDD induced the directional migration of human neuroblastoma cells in a time- and concentration-dependent manner, and AhR was confirmed to mediate this process. The AhR-mediated mRNA and miR expressions involved in the axon guidance pathway played an important role in the migration of human neuroblastoma cells. Our study provided helpful insights into the systematic and comprehensive understanding of the mechanism of action of dioxins on human neuroblastoma cells.

CRediT authorship contribution statement

Tuan Xu: Methodology, Software, Validation, Formal analysis, Investigation, Data curation, Writing – original draft, Writing – review & editing, Visualization. **Yali Luo:** Validation, Formal analysis, Investigation, Data curation, Writing – review & editing. **Heidi Qunhui Xie:** Conceptualization, Methodology, Resources, Data curation, Writing – original draft, Writing – review & editing, Supervision, Project administration, Funding acquisition. **Yingjie Xia:** Validation, Investigation, Data curation, Writing – review & editing. **Yunping Li:** Validation, Investigation, Data curation, Writing – review & editing. **Yangsheng Chen:** Investigation, Writing – review & editing. **Zhiling Guo:** Investigation, Writing – review & editing. **Li Xu:** Data curation, Writing – review & editing. **Bin Zhao:** Conceptualization, Resources, Supervision, Project administration, Funding acquisition, Writing – review & editing.

Declaration of Competing Interest

The authors declare that they have no known competing financial interests or personal relationships that could have appeared to influence the work reported in this paper.

Data availability

Data will be made available on request.

Acknowledgement

Appendix A. Supplementary material

Primers for Real-Time RT-PCR Analysis; Initial area and width of the wounds; Additional migration distance of TCDD-treated groups compared to controls; List of differentially expressed genes; KEGG pathways based on the upregulated genes; GO terms based on the upregulated genes.; KEGG pathways based on the downregulated genes; GO terms based on the downregulated genes; The information of miRs-migration related genes pairs; All genes were involved in the axon guidance pathway; Characteristics analysis of the axon guidance pathway related down regulated genes. Schematic map for cell migration process caused by TCDD. (PDF). Supplementary data to this article can be found online at https://doi.org/10.1016/j.envint.2022.107461.

References

Beischlag, T.V., Morales, J.L., Hollingshead, B.D., Perdew, G.H., 2008. The aryl hydrocarbon receptor complex and the control of gene expression. Crit. Rev. Eukaryot. Gene Expr. 18 (3), 207–250.

Bui, L.-C., Tomkiewicz, C., Chevallier, A., Pierre, S., Bats, A.-S., Mota, S., Raingeaud, J., Pierre, J., Diry, M., Transy, C., Garlatti, M., Barouki, R., Coumoul, X., 2009. Nedd9/Hef1/Cas-L mediates the effects of environmental pollutants on cell migration and plasticity. Oncogene 28 (41), 3642–3651.

Diry, M., Tomkiewicz, C., Koehle, C., Coumoul, X., Bock, K.W., Barouki, R., Transy, C., 2006. Activation of the dioxin/aryl hydrocarbon receptor (AhR) modulates cell plasticity through a JNK-dependent mechanism. Oncogene 25 (40), 5570–5574.

Erkutlu, I., Cigiloglu, A., Kalender, M.E., Alptekin, M., Demiryurek, A.T., Suner, A., Ozkaya, E., Ulaslı, M., Camcı, C., 2013. Correlation between Rho-kinase pathway gene expressions and development and progression of glioblastoma multiforme. Tumor Biol. 34 (2), 1139–1144.

Eskenazi, B., Mocarelli, P., Warner, M., Samuels, S., Vercellini, P., Olive, D., Needham, L. L., Patterson, D.G., Brambilla, P., Gavoni, N., Casalini, S., Panazza, S., Turner, W., Gerthoux, P.M., 2002. Serum dioxin concentrations and endometriosis: a cohort study in Seveso, Italy. Environ. Health Perspect. 110 (7), 629–634.

Evans, I.M., Yamaji, M., Britton, G., Pellet-Many, C., Lockie, C., Zachary, I.C., Frankel, P., 2011. Neuropilin-1 signaling through p130Cas tyrosine phosphorylation is essential for growth factor-dependent migration of glioma and endothelial cells. Mol. Cell. Biol. 31 (6), 1174–1185.

Frueh, F.W., Hayashibara, K.C., Brown, P.O., Whitlock, J.P., 2001. Use of cDNA microarrays to analyze dioxin-induced changes in human liver gene expression. Toxicol. Lett. 122 (3), 189–203.

Fujita, H., Samejima, H., Kitagawa, N., Mitsuhashi, T., Washio, T., Yonemoto, J., Tomita, M., Takahashi, T., Kosaki, K., 2006. Genome-wide screening of dioxin-responsive genes in fetal brain: bioinformatic and experimental approaches. Congenit Anom (Kyoto) 46 (3), 135–143.

Gandhi, D., Sivanesan, S., Kannan, K., 2018. Manganese-Induced Neurotoxicity and Alterations in Gene Expression in Human Neuroblastoma SH-SY5Y Cells. Biol. Trace Elem. Res. 183 (2), 245–253.

Hanieh, H., 2015. Aryl hydrocarbon receptor-microRNA-212/132 axis in human breast cancer suppresses metastasis by targeting SOX4. Mol. Cancer 14, 1–13.

He, Y.i., Li, H.-L., Xie, W.-Y., Yang, C.-Z., Yu, A.C.H., Wang, Y., 2007. The presence of active Cdk5 associated with p35 in astrocytes and its important role in process elongation of scratched astrocyte. Glia 55 (6), 573–583.

Jia, H., Cheng, L., Tickner, M., Bagherzadeh, A., Selwood, D., Zachary, I., 2010. Neuropilin-1 antagonism in human carcinoma cells inhibits migration and enhances chemosensitivity. Br. J. Cancer 102 (3), 541–552.

Jimma, Y., Jimma, K., Yachi, M., Hakata, S., Habano, W., Ozawa, S., Terashima, J., 2019. Aryl hydrocarbon receptor mediates cell proliferation enhanced by Benzo [a] pyrene in human lung cancer 3D spheroids. Cancer Invest. 37 (8), 367–375.

Jin, U.-H., Lee, S.-O., Pfent, C., Safe, S., 2014. The aryl hydrocarbon receptor ligand omeprazole inhibits breast cancer cell invasion and metastasis. BMC Cancer 14, 1–14.

Kerr, M.A., Nasca, P.C., Mundt, K.A., Michalek, A.M., Baptiste, M.S., Mahoney, M.C., 2000. Parental occupational exposures and risk of neuroblastoma: a case-control study (United States). Cancer Causes Control: CCC 11, 635–643.

Kim, S.M., Han, D.H., Lyoo, H.S., Min, K.J., Kim, K.H., Renshaw, P., 2010. Exposure to environmental toxins in mothers of children with autism spectrum disorder. Psychiatry Investig. 7, 122–127.

Li, Y., Wang, K., Jiang, Y.-Z., Chang, X.-W., Dai, C.-F., Zheng, J., 2014. 2, 3, 7, 8-Tetrachlorodibenzo-p-dioxin (TCDD) inhibits human ovarian cancer cell proliferation. Cellular Oncol. 37 (6), 429–437.

Li, Z., Yu, X., Wang, Y., Shen, J., Wu, W.K.K., Liang, J., Feng, F., 2015. By downregulating TIAM1 expression, microRNA-329 suppresses gastric cancer invasion and growth. Oncotarget 6 (19), 17559–17569.

Long, C., Jiang, L., Wei, F., Ma, C., Zhou, H., Yang, S., Liu, X., Liu, Z., Maas, S., 2013. Integrated miRNA-mRNA analysis revealing the potential roles of miRNAs in chordomas. PLoS ONE 8 (6), e66676.

Luo, Y., Xu, T., Xie, H.Q., Guo, Z., Zhang, W., Chen, Y., Sha, R., Liu, Y., Ma, Y., Xu, L.i., Zhao, B., 2020. Effects of 2,3,7,8-tetrachlorodibenzo-p-dioxin on spontaneous movement of human neuroblastoma cells. Sci. Total Environ. 715, 136805.

McHale, C.M., Zhang, L., Hubbard, A.E., Zhao, X., Baccarelli, A., Pesatori, A.C., Smith, M. T., Landi, M.T., 2007. Microarray analysis of gene expression in peripheral blood mononuclear cells from dioxin-exposed human subjects. Toxicology 229 (1-2), 101–113.

Mitsui, T., Taniguchi, N., Kawasaki, N., Kagami, Y., Arita, J., 2011. Fetal exposure to 2,3,7,8-tetrachlorodibenzo-p-dioxin induces expression of the chemokine genes Cxcl4 and Cxcl7 in the perinatal mouse brain. J. Appl. Toxicol.: JAT 31 (3), 279–284.

Pang, W., Lian, F.-Z., Leng, X., Wang, S.-M., Li, Y.-b., Wang, Z.-y., Li, K.-R., Gao, Z.-X., Jiang, Y.-G., 2018. Microarray expression profiling and co-expression network analysis of circulating LncRNAs and mRNAs associated with neurotoxicity induced by BPA. Environ. Sci. Pollut. Res. Int. 25 (15), 15006–15018.

Park, J.R., Eggert, A., Caron, H., 2010. Neuroblastoma: biology, prognosis, and treatment. Hematol. Oncol. Clin. North Am. 24 (1), 65–86.

Peng, T.-L., Chen, J., Mao, W., Song, X., Chen, M.-H., 2009. Aryl hydrocarbon receptor pathway activation enhances gastric cancer cell invasiveness likely through a c-Jun-dependent induction of matrix metalloproteinase-9. BMC Cell Biol. 10, 1–7.

Perepechaeva, M.L., Grishanova, A.Y., 2020. The role of aryl hydrocarbon receptor (AHR) in brain tumors. Int. J. Mol. Sci. 21, 2863.

Ru, Y., Kechris, K.J., Tabakoff, B., Hoffman, P., Radcliffe, R.A., Bowler, R., Mahaffey, S., Rossi, S., Calin, G.A., Bemis, L., 2014. The multiMiR R package and database: integration of microRNA-target interactions along with their disease and drug associations. Nucleic Acids Res. 42, e133.

Seifert, A., Rau, S., Küllertz, G., Fischer, B., Santos, A.N., 2009. TCDD induces cell migration via NFATc1/ATX-signaling in MCF-7 cells. Toxicol. Lett. 184, 26–32.

The Tai, P., Nishijo, M., Kido, T., Nakagawa, H., Maruzeni, S., Naganuma, R., Thi Nguyet Anh, N., Morikawa, Y., Luong, H.V., Anh, T.H., Hung, N.N., Son, L.K., Tawara, K., Nishijo, H., 2011. Dioxin concentrations in breast milk of Vietnamese nursing mothers: a survey four decades after the herbicide spraying. Environ. Sci. Technol. 45 (15), 6625–6632.

Van Battum, E.Y., Brignani, S., Pasterkamp, R.J., 2015. Axon guidance proteins in neurological disorders. Lancet Neurol. 14 (5), 532–546.

Van der Goten, J., Vanhove, W., Lemaire, K., Van Lommel, L., Machiels, K., Wollants, W.-J., De Preter, V., De Hertogh, G., Ferrante, M., Van Assche, G., Rutgeerts, P., Schuit, F., Vermeire, S., Arijs, I., Chamaillard, M., 2014. Integrated miRNA and mRNA expression profiling in inflamed colon of patients with ulcerative colitis. PLoS ONE 9 (12), e116117.

Villano, C., Murphy, K., Akintobi, A., White, L., 2006. 2, 3, 7, 8-tetrachlorodibenzo-p-dioxin (TCDD) induces matrix metalloproteinase (MMP) expression and invasion in A2058 melanoma cells. Toxicol. Appl. Pharmacol. 210 (3), 212–224.

Vogel, C.F., Sciullo, E., Matsumura, F., 2004. Activation of inflammatory mediators and potential role of ah-receptor ligands in foam cell formation. Cardiovasc. Toxicol. 4, 363–373.

Wang, Z., Xue, Y., Wang, P., Zhu, J., Ma, J., 2016. MiR-608 inhibits the migration and invasion of glioma stem cells by targeting macrophage migration inhibitory factor. Oncol. Rep. 35, 2733–2742.

Xia, X., Zhang, K., Cen, G., Jiang, T., Cao, J., Huang, K., Huang, C., Zhao, Q., Qiu, Z., 2015. MicroRNA-301a-3p promotes pancreatic cancer progression via negative regulation of SMAD4. Oncotarget 6 (25), 21046–21063.

Xie, H.Q., Xu, H.-M., Fu, H.-L., Hu, Q., Tian, W.-J., Pei, X.-H., Zhao, B., 2013. AhR-mediated effects of dioxin on neuronal acetylcholinesterase expression in vitro. Environ. Health Perspect. 121 (5), 613–618.

Xu, T., Xie, H.Q., Li, Y., Xia, Y., Chen, Y., Xu, L., Wang, L., Zhao, B., 2017. CDC42 expression is altered by dioxin exposure and mediated by multilevel regulations via AhR in human neuroblastoma cells. Sci. Rep. 7, 1–10.

Xu, T., Xie, H.Q., Li, Y., Xia, Y., Sha, R., Wang, L., Chen, Y., Xu, L.i., Zhao, B., 2018. Dioxin induces expression of hsa-miR-146b-5p in human neuroblastoma cells. J. Environ. Sci. (China) 63, 260–267.

Xue, P., Fu, J., Zhou, Y., 2018. The aryl hydrocarbon receptor and tumor immunity. Front. Immunol. 9, 286.

Yamaguchi, M., Hankinson, O., 2019. 2, 3, 7, 8-tetrachlorodibenzo-p-dioxin suppresses the growth of human colorectal cancer cells in vitro: Implication of the aryl hydrocarbon receptor signaling. Int. J. Oncol. 54, 1422–1432.

Yin, F., Zhang, J.N., Wang, S.W., Zhou, C.H., Zhao, M.M., Fan, W.H., Fan, M., Liu, S., Lee, S.-G., 2015. MiR-125a-3p regulates glioma apoptosis and invasion by regulating Nrg1. PLoS ONE 10 (1), e0116759.

Yu, G., Wang, L.-G., Han, Y., He, Q.-Y., 2012. clusterProfiler: an R package for comparing biological themes among gene clusters. OMICS 16 (5), 284–287.

Zhang, L., Zhang, Y.i., Zhu, H., Sun, X., Wang, X., Wu, P., Xu, X., 2019. Overexpression of miR-301a-3p promotes colorectal cancer cell proliferation and metastasis by

targeting deleted in liver cancer-1 and runt-related transcription factor 3. J. Cell. Biochem. 120 (4), 6078–6089.

Zhao, B., Degroot, D.E., Hayashi, A., He, G., Denison, M.S., 2010. CH223191 is a ligand-selective antagonist of the Ah (Dioxin) receptor. Toxicol. Sci.: An Official J. Soc. Toxicol. 117, 393–403.

Zhu, P., Zhou, K., Lu, S., Bai, Y.u., Qi, R., Zhang, S., 2020. Modulation of aryl hydrocarbon receptor inhibits esophageal squamous cell carcinoma progression by repressing COX2/PGE2/STAT3 axis. J. Cell Commun. Signaling 14 (2), 175–192.